

PACS numbers: 42.62.Be; 87.64.Cc; 87.63.L–
DOI: 10.1070/QE2010v040n12ABEH014505

Blood oxygenation monitoring by diffuse optical tomography

M. Patachia, D.C.A. Dutu, D.C. Dumitras

Abstract. **Diffuse optical tomography (DOT) makes it possible to reconstruct, in two or three dimensions, the internal structure of the biological tissues based on the distribution of the absorption coefficient and the reduced scattering coefficient, using optical measurements at multiple source–detector positions on the tissue surface. The measurement of the light intensity transmitted through the tissue can be also used to compute the haemoglobin and oxyhaemoglobin concentrations, measuring the selective absorption of the main blood chromophores by near infrared spectroscopy (NIRS). The spectral selectivity of the system and the evaluation of the blood volume and blood oxygenation (BV and OXY distributions), together with the reconstruction of the inner structure of the tissue, can improve the accuracy of early cancer diagnosis, based on the tissue angiogenesis characterisation.**

Keywords: *diffuse optical tomography, near infrared spectroscopy, blood phantom, oxyhaemoglobin concentration.*

1. Introduction

The multispectral diffuse optical tomography (DOT) enables the non-invasive reconstruction of the internal tissue structure and the evaluation of the main chromophore concentration in the tissue. In this paper, we investigate the ability of a simple multispectral continuous-wave DOT system (cw-DOT) [1] to evaluate, using the NIRS, the concentration of the main chromophores in the tissue, namely: haemoglobin and oxyhaemoglobin.

In comparison with the main works [2–4] which describe the measurement of the blood volume (BV) and oxygenation (OXY) distribution in tissues, the use of the modulated laser light and its spectral accuracy has enable us not only to reduce the noise in the spectral measurements but also to evaluate the chromophore distribution in the measuring plane through multiple source–receiver light pair.

The main advantage of the cw-DOT system in comparison with blood oximetry systems based on NIRS is its ability to measure directly the absorption coefficient (μ_a) and the reduced scattering coefficient (μ_s') and also a wide range of functional contrasts such as oxyhaemoglobin (HbO_2), deoxyhaemoglobin (Hb), and blood volume, which increases the diagnostic accuracy based on angiogenesis in the pathological zone [5, 6].

To illustrate the scheme and investigate its feasibility, we have developed a simple blood phantom based on intralipid and human blood.

M. Patachia Department of Lasers, National Institute for Laser, Plasma and Radiation Physics, 409 Atomistilor St., P.O. Box MG-36, 077125, Bucharest, Romania; Faculty of Physics, University of Bucharest, 405 Atomistilor St., P.O. Box MG-11, 077125, Bucharest, Romania; e-mail: mihai.patachia@inflpr.ro;
D.C.A. Dutu, D.C. Dumitras Department of Lasers, National Institute for Laser, Plasma and Radiation Physics, 409 Atomistilor St., P.O. Box MG-36, 077125, Bucharest, Romania; e-mail: doru.dutu@inflpr.ro

Received 28 October 2010
Kvantovaya Elektronika **40** (12) 1062–1066 (2010)
Submitted in English

2. cw-NIRS instrumentation

For our cw-NIRS experiments we have used an inexpensive continuous-wave DOT system [1] containing two spatially combined Roithner Lasertechnik laser diodes (RLT780-1000G; 1 W at 785 nm and RLT83500G, 0.5 W at 830 nm), a variable-gain OE-200-SI photodetector equipped with a Si photodiode 1.2 mm in diameter, and two LIA-MV-150 lock-in amplifiers (FEMTO Messtechnik GmbH). The system can perform 128 independent measurements in about 60 seconds through two time-division-multiplexed optic schemes with eight illumination (S) fibres and eight detector (R) fibres in the measuring head (optode) (Fig. 1).

The serial activation of a given light source (S_i) in the measuring head is possible through an optical DMUX demultiplexer (single-input, multiple-output switch) connected to a PI M505.2S2 translation stage (Mercury Inc.), which moves the collimator connected to the optical coupler of two laser diodes and precisely sets its position in front of the illumination fibres.

The light transmitted through the target media (tissue phantom) is measured using a similar serial approach but through an optical MUX multiplexer (multiple-input, single-output switch), which moves precisely in front of the detecting fibres (R_i); the collimator is placed at the input of the photo preamplifier. A microprocessor-controlled stepper M505.2S2 motor (20000 counts rev.$^{-1}$) providing ultrasmooth (vibration-free) motion (with a minimum incremental of 0.1 μm), allows a relatively fast and precise positioning of the collimator in front of the illumination/measuring fibres in a 50-mm travel range.

This complex structure enables us to investigate the dependence of the signal on the distance between the light source and receiver and to perform dynamic spectral measurements when the system uses eight special distributed light sources and eight receivers.

A liquid phantom simulating the optical properties of the tissue was used to test the efficiency of the system. The basis of the phantom was formed by a scattering solution of intralipid (Lipofundin) and water with an overall reduced scattering coefficient of $\mu_s' = 0.8$ mm^{-1} (the wavelength of 785 nm).

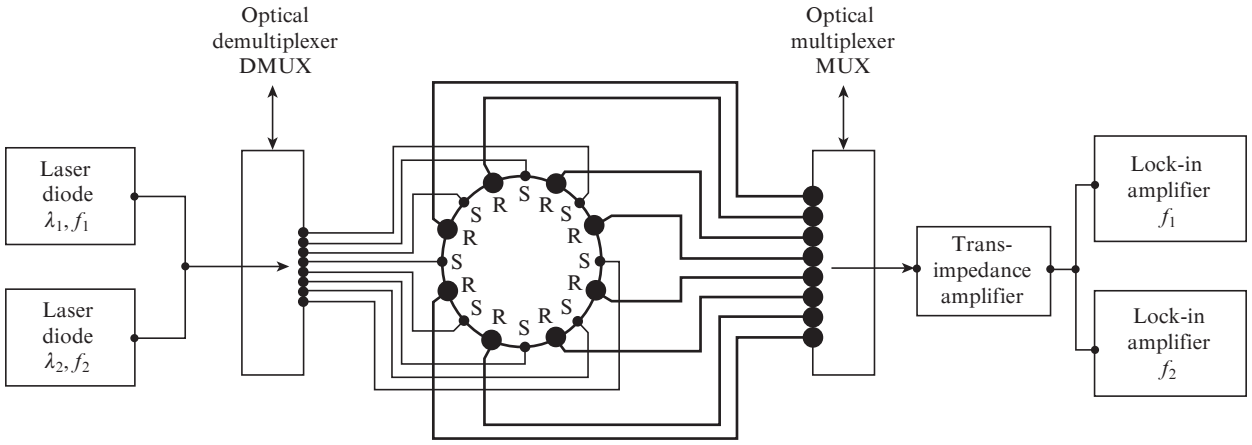

Figure 1. A cw-DOT setup used for monitoring blood oxygenation.

To obtain the desired scattering coefficient, the dilution follows the formula:

$$\mu_s'^{\text{bef}} V^{\text{bef}} + \mu_s'^{\text{intr}} V^{\text{intr}} = \mu_s'^{\text{aft}} V^{\text{aft}}, \tag{1}$$

where V is the solution volume and the superscripts 'bef' and 'aft' refer to the initial and final stages of the dilution process. The solution was placed in a cylindrical beaker and a magnetic stirring rod was used to maintain the homogeneity during the experiment for the dynamic regime.

Healthy human blood treated with sodium citrate was added to the scattering solution to achieve a volume fraction of 1.5% haemoglobin, or a total concentration of 30 μM. This is a typical value for normal physiological conditions with an assumption that the fraction of the blood volume is 1.5% and that of hematocrit is 15%. The blood was delivered by a specialised laboratory in order to ensure all the physicochemical properties of the samples.

To induce deoxygenation in the liquid phantom, 4 g of baker's yeast was added to the solution. The temperature of the phantom was maintained at 37 °C during the deoxygenation process to keep the yeast active. To avoid mechanical hemolysis during our experiments, we used a round-head stirring rod and the frequency of the stirring process was kept between 100 and 200 rpm.

Deoxygenation was observed until haemoglobin saturation reached a steady state at 25%. When deoxygenation of the yeast–intralipid solution reached a steady state, oxygenation was simulated again by delivering a slow oxygen flux to the phantom from an oxygen tank. The oxygen supply was maintained until a steady state level of oxygenation was obtained. The steady-state haemoglobin saturation was 85%.

3. Principles of cwNIRS measurement device

According to the modified Beer–Lambert law (MBLL), the optical density (OD) variation ΔOD (dimensionless quantity) at time t due to variations in concentrations of oxyhaemoglobin ΔC_{HbO_2} and deoxyhaemoglobin ΔC_{Hb} (in μM) is described as

$$\Delta\text{OD}(r,s;\lambda,t) = -\ln\frac{I(r,s;\lambda,t)}{I_0(r,s;\lambda)}$$

$$= [\varepsilon_{\text{HbO}_2}(\lambda)\Delta C_{\text{HbO}_2}(r;t) + \varepsilon_{\text{Hb}}(\lambda)\Delta C_{\text{Hb}}(r;t)]\text{DPF}(r)d(r), \tag{2}$$

where r, s are the coordinates of the detector and source position; λ is the wavelength of the laser source; $I(r,s;\lambda,t)$ is the measured photon flux at time t; $I_0(r,s;\lambda)$ is the initial photon flux; $\varepsilon_{\text{HbO}_2}(\lambda)$ and $\varepsilon_{\text{Hb}}(\lambda)$ (in $\mu\text{M}^{-1}\ \text{mm}^{-1}$) are the extinction coefficients of the HbO_2 and Hb, respectively; DPF(r) is the dimensionless differential pathlength factor; and $d(r)$ (in mm) is the distance between the source and the detector at the position r [2, 7].

OD_λ can be defined as the attenuation in the light intensity at the wavelength λ. This attenuation is the superposition of optical losses of light absorption (A_λ) and scattering (S_λ). The MBLL indicates that HbO_2 and Hb concentration variations can be estimated using the optical density measurements at two wavelengths. Then, the HbX (i.e., HbO_2 or Hb) concentration variations are then obtained from

$$\Delta C_{\text{Hb}X}(r_i,s_i;t) = \frac{\Delta\text{OD}_{\text{Hb}X}(r_i,s_i;t)}{\text{DPF}(r)d(r)}. \tag{3}$$

As the distances between the source and detector are relatively large, and the haemoglobin concentration variations could be at any point between the source and detector, some ambiguities are present in the above calculated HbX variation [Eqn (3)].

Taking into account the contributions of the two chromophores, equation (2) can be rewritten in the form:

$$\Delta\text{OD}_\lambda = (\varepsilon_{\lambda\,\text{HbO}_2}\Delta C_{\text{HbO}_2} + \varepsilon_{\lambda\,\text{Hb}}\Delta C_{\text{Hb}})\text{DPF}_\lambda d. \tag{4}$$

By measuring ΔOD_λ at two wavelengths (λ_1 and λ_2) and using the known extinction coefficients of oxyhaemoglobin ($\varepsilon_{\text{HbO}_2}$) and deoxyhaemoglobin ($\varepsilon_{\text{Hb}}$) at these wavelengths, we can determine their concentration variations:

$$\Delta C_{\text{Hb}} = \left(\varepsilon_{\lambda_2\text{HbO}_2}\frac{\Delta\text{OD}_{\lambda_1}}{\text{DPF}_{\lambda_1}} - \varepsilon_{\lambda_1\text{HbO}_2}\frac{\Delta\text{OD}_{\lambda_2}}{\text{DPF}_{\lambda_2}}\right)$$

$$\times[(\varepsilon_{\lambda_1\text{Hb}}\varepsilon_{\lambda_2\text{HbO}_2} - \varepsilon_{\lambda_2\text{Hb}}\varepsilon_{\lambda_1\text{HbO}_2})d]^{-1}, \tag{5}$$

$$\Delta C_{\text{HbO}_2} = \left(\varepsilon_{\lambda_1\text{Hb}}\frac{\Delta\text{OD}_{\lambda_2}}{\text{DPF}_{\lambda_2}} - \varepsilon_{\lambda_2\text{HbO}_2}\frac{\Delta\text{OD}_{\lambda_1}}{\text{DPF}_{\lambda_1}}\right)$$

$$\times[(\varepsilon_{\lambda_1\text{Hb}}\varepsilon_{\lambda_2\text{HbO}_2} - \varepsilon_{\lambda_2\text{Hb}}\varepsilon_{\lambda_1\text{HbO}_2})d]^{-1}. \tag{6}$$

Assuming that concentration variations are both global and small and using for DPF_λ the relation

$$DPF_\lambda = \frac{1}{2}\left(\frac{3\mu_{s\lambda}}{\mu_{a\lambda}^{init}}\right)^{1/2}\left[1 - \frac{1}{1 + d(3\mu_{s\lambda}^{init}\mu_{a\lambda}^{init})^{1/2}}\right], \quad (7)$$

we obtain the solution of the photon diffusion equation for a semi-infinite medium:

$$\Delta OD_\lambda = \frac{1}{2}\left(\frac{3\mu_{s\lambda}}{\mu_{a\lambda}^{init}}\right)^{1/2}\left[1 - \frac{1}{1 + d(3\mu_{s\lambda}^{init}\mu_{a\lambda}^{init})^{1/2}}\right]$$

$$\times(\varepsilon_{\lambda HbO_2}\Delta C_{HbO_2} + \varepsilon_{\lambda Hb}\Delta C_{Hb})d. \quad (8)$$

This relation shows that ΔOD_λ depends on the tissue scattering, initial chromophore concentration, extinction coefficient, and optode separation d.

Information about the blood chromophores can be used to estimate the blood volume and tissue oxygenation which are indications of the hemodynamic activity.

Different approaches can be used to implement NIRS such as time-resolved, frequency-domain, and continuous-wave techniques. Among these methods, cw-NIRS is the most practical one, where light with a constant amplitude is injected into the tissue, then the decay of the light intensity amplitude due to the absorption is analysed. The changes in the light amplitude are used to calculate variations in the concentrations of the blood chromophores. Due to its practicality, cw-NIRS systems allow bedside monitoring of blood chromophores for extended periods.

Because each chromophore has a specific extinction coefficient and a differential pathlength factor, the measurement with two wavelengths can be simply expressed by a matrix system (T stands for transposed matrix), namely:

$$\overline{\Delta OD} = \overline{M} \times \overline{\Delta C}, \quad (9)$$

where

$$\overline{\Delta OD} = \begin{vmatrix} \Delta OD_{\lambda_1} \\ \Delta OD_{\lambda_2} \end{vmatrix}; \quad \overline{\Delta C} = \begin{vmatrix} \Delta C_{HbO_2} \\ \Delta C_{Hb} \end{vmatrix};$$

$$\overline{M} = d\left(\begin{vmatrix} \varepsilon_{\lambda_1 HbO_2} & \varepsilon_{\lambda_2 HbO_2} \\ \varepsilon_{\lambda_1 Hb} & \varepsilon_{\lambda_2 Hb} \end{vmatrix}\begin{vmatrix} DPF_{\lambda_1} & 0 \\ 0 & DPF_{\lambda_2} \end{vmatrix}\right)^T.$$

Therefore, equation (9) establishes the relationship between the changes in the light intensity and blood chromophore concentrations.

Let us find the two parameters as functions of the blood chromophore concentrations, namely:

$$BV = \Delta C_{HbO_2} + \Delta C_{Hb}, \quad (10)$$

$$OXY = \Delta C_{HbO_2} - \Delta C_{Hb}, \quad (11)$$

which are assumed proportional to variations in the blood volume and oxygenation in the tissue due to the hemodynamic activation.

4. Calculation and parameters

The absorption and reduced scattering coefficients used in the calculation of the DPF_λ employ the values given in the literature [8]. Assuming that the oxygen saturation level amounts to 85% and the total haemoglobin concentration – to 150 μM, we obtain the following absorption and reduced scattering coefficients: $\mu_{a785} = 0.016$ mm^{-1}, $\mu_{a830} = 0.022$ mm^{-1}, $\mu'_{s785} = 0.8$ mm^{-1}, $\mu'_{s830} = 0.95$ mm^{-1}.

Substituting these coefficients into (7), we obtain the DPF_λ values for different distances d between the light source and receiver at the two specified wavelength (see Table 1). These values are consistent with the measurements from literature [3]. In addition, using data in the literature [8] we obtain:

$$\bar{\varepsilon} = \begin{vmatrix} \varepsilon_{HbO_2}^{785} & \varepsilon_{HbO_2}^{830} \\ \varepsilon_{Hb}^{785} & \varepsilon_{Hb}^{830} \end{vmatrix} = \begin{vmatrix} 0.731 & 0.974 \\ 0.997 & 0.693 \end{vmatrix}. \quad (12)$$

Table 1. DPF_λ for different distances d between the light source and receiver.

d/mm	DPF_{785}	DPF_{830}
9.75	4.02	4.04
19.13	4.83	4.70
27.7	5.17	4.98

Substituting (12) into equation (9), we derive the relationship between light intensity variation and blood chromophore concentration for different d:

$$\begin{vmatrix} \Delta C_{HbO_2} \\ \Delta C_{Hb} \end{vmatrix} = \begin{vmatrix} -0.38066 & 0.53502 \\ 0.54528 & -0.39980 \end{vmatrix}\begin{vmatrix} \Delta OD_{785} \\ \Delta OD_{830} \end{vmatrix},$$

$d = 9.75$ мм;

$$\begin{vmatrix} \Delta C_{HbO_2} \\ \Delta C_{Hb} \end{vmatrix} = \begin{vmatrix} -0.16330 & 0.226746 \\ 0.23831 & -0.17473 \end{vmatrix}\begin{vmatrix} \Delta OD_{785} \\ \Delta OD_{830} \end{vmatrix}, \quad (13)$$

$d = 19.13$ мм;

$$\begin{vmatrix} \Delta C_{HbO_2} \\ \Delta C_{Hb} \end{vmatrix} = \begin{vmatrix} -0.10385 & 0.14596 \\ 0.15534 & -0.11390 \end{vmatrix}\begin{vmatrix} \Delta OD_{785} \\ \Delta OD_{830} \end{vmatrix},$$

$d = 27.75$ мм.

5. Results and discussion

A dynamic liquid phantom simulating the optical properties of the tissue was used to test the efficiency of the system. The solution was placed in a special cylindrical beaker with an oxygen supply pipe in the lower part. The oxygen pipe was closed by a porous glass wall which prevented the penetration of the liquid in the oxygen pipe line and improved the oxygen bubbles distribution in the liquid phantom volume.

Deoxygenation and oxygenation of the haemoglobin was successively realised by immersing a small yeast bag in the liquid phantom and then delivering extra oxygen to the phantom from an oxygen tank. The oxygen supply was maintained until a steady-state level of oxygenation was obtained.

The yeast was placed in a filter beg to avoid its mixture in the liquid phantom and the mud formation. This precaution is valid only for a few deoxygenation cycles.

The signal evolution proportional to the photon flux was measured at the output of the two lock-in amplifiers for each wavelength. The signal measured by the receiving photodetector which was placed at the distance d from the light source describes the chromophore concentration during the oxygenation and deoxygenation processes in the blood phantom (Fig. 2).

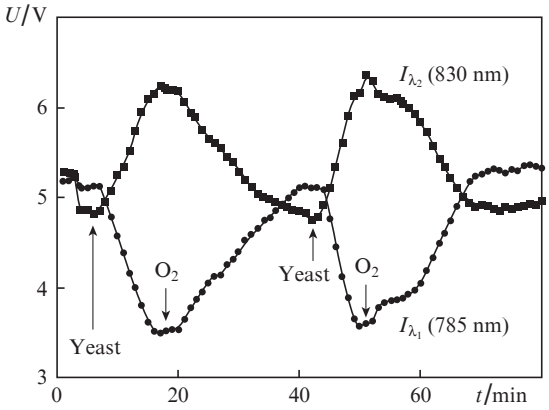

Figure 2. Voltage at the output of two lock-in amplifiers, used to decode the signal, at 785 and 830 nm.

Knowing the signal measured at the output of the two lock-in amplifiers, the laser powers at the output of the illuminating fibre (6.61 mW for 785 nm and 19.1 mW for 830 nm) and the total gain in the measuring system, we can compute according to the equations (2), (9) and (12), the oxy and deoxyhaemoglobin concentrations (Fig. 3).

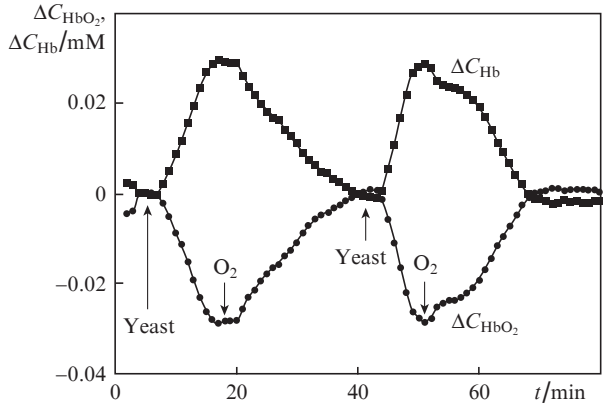

Figure 3. Time evolution of the oxyhaemoglobin and deoxyhaemoglobin concentration in the tissue phantom under the hemodynamic activation through the oxygen flow and yeast adding.

For known values of C_{HbO_2} and C_{Hb}, according to equations (10) and (11), the oxygenation (OXY) and the blood volume (BV) can be evaluated (Fig. 4). The measured data are in good agreement with the main results published in the literature in the last years [3, 4, 5].

During the measurements the variations in haemoglobin and oxyhaemoglobin concentration can be observed from the colour of the liquid phantom which changes from bright red for full oxygenation to dark red for full deoxygenation. The reduced hemolysis in the blood phantom is confirmed by the

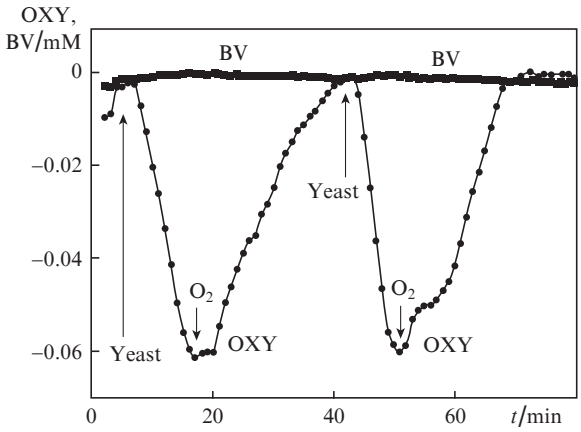

Figure 4. Time evolution of the oxygenation and blood volume under the hemodynamic activation through the oxygen flow and yeast adding.

reproducibility of the saturation level for haemoglobin, which remain constant during our cyclic measurements (85%).

The same result is obtained also if the concentration is measured dynamically using eight pairs of sources and detectors in the measuring head and software which initiates periodic connection of two optical multiplexer in the measuring system of each adjacent source–detector pair (S_iR_i). The distance between the light source and receiver in the pair (S_iR_i) is 9.75 mm as in the static measurements.

When calculating ΔOD_λ, it is necessary to introduce a correction factor to compensate for the errors in the alignment of the optical fibre in two optical multiplexers and the measuring head. The correction factor is given by the scaling factor of the signal in the intralipid solution for eight light source–receiver pairs.

The time dependence of OXY and BV under the hemodynamic activation is presented in Fig. 5.

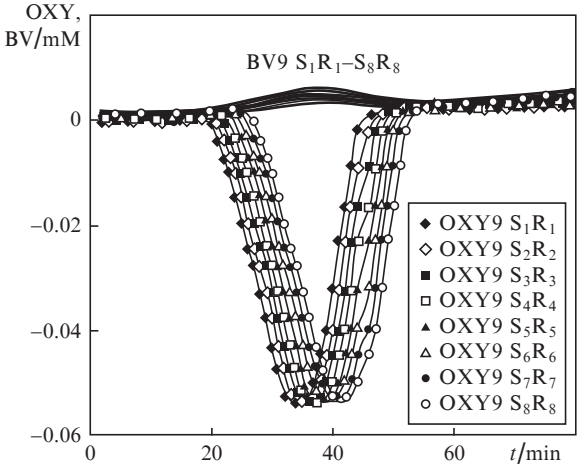

Figure 5. Time evolution of the oxygenation and blood volume under the hemodynamic activation and using the dynamic data acquisition of the DOT system.

6. Conclusions

The obtained results confirm the design parameters of the liquid phantom and the ability of the system to evaluate the haemoglobin and oxyhaemoglobin concentration.

The good agreement of the static and dynamic measurements demonstrates the homogeneity of the liquid phantom. The measurements present less than 5% variations in the measurements, which is due to the oxygen bubbles flowing in solution during the oxygenation process and to the yeast mud resulting from the insertion of the yeast bag in the liquid phantom.

The use of the laser diodes for illuminating biological tissues instead of LED sources increases the signal-to-noise ratio and makes it possible to develop a complex setup with multiple source–receiver pairs. Application of the NIRS algorithms along with the DOT image reconstruction techniques improves the tissue characterisation, because NIRS is the only method that can potentially measure hemodynamic metabolism and neuronal signals simultaneously. The laser light improves the spectral selectivity and the spatiotemporal resolution and allows one to avoid the increase in the tissue temperature at the contact between the surface and the light source.

The main advantage of the functional NIRS is that allows one to measure directly a wide range of such functional contrasts as oxyhaemoglobin, deoxyhaemoglobin, and total haemoglobin with a very high temporal resolution. The chromophore distribution analysis through cw-NIRS can enhance the resolution and accuracy in various deep-tissue applications of the cw-DOT, including breast cancer imaging [6].

References

1. Dutu D.C.A., Dumitras D.C., Matei C., Magureanu A.M., Patachia M., Miclos S., Savastru D., Liang X., Jiang H., Iftimia N., *Design and Parametric Evaluation of a Continuous-wave Diffuse Optical Tomography System* (ICPEPA'09) (Sapporo, Japan, 2009).
2. Chul Ye J., Tak S., Eun Jang K., Jung J., Jang J. *Neuroimage*, **44**, 428 (2009).
3. Bozkurt A., Rosen A., Rosen H., Onaral B. *A Portable Near Infrared Spectroscopy System for Bedside Monitoring of Newborn Brain*, *BioMedical Eng. OnLine* (2005).
4. Hazinski M.F. *Pediatric Evaluation and Monitoring Considerations*, *Hemodynamic Monitoring: Invasive and Noninvasive Clinical Application*, Ed. by G.O.Darovic (Philadelphia, PA: W.B.Saunders, 2002) pp 471–514.
5. Devaraj A. *Signal Processing for Functional Near-infrared Neuroimaging*, PhD Thesis, Drexel University, 2005.
6. Srinivasan S., Pogue B.W., Jiang S.D., Dehghani H., Kogel C., Soho S., Gibson J.J., Tosteson T.D., Poplack S.P., Paulsen K.D. *Proc. Nat. Acad. Sci. USA*, **100**, 12349 (2003).
7. Heiskala J., Kotilahti K., Nissilä I. *Proc. 2005 IEEE Eng. in Medicine and Biology 27th Annual Conf.* (Shanghai, China, 2005).
8. Prahl S. *Tabulated Molar Extinction Coefficient for Hemoglobin in Water* (prahl@ece.ogi.edu).